Bleaching and stimulated recovery of dyes and of photocantilevers

D. Corbett and M. Warner*
Cavendish Laboratory, Madingley Road, Cambridge, CB3 0HE, United Kingdom
(Received 14 February 2008; published 30 May 2008)

We examine how intense optical beams can penetrate deeply into highly absorbing media by a nonlinear, photobleaching process. The role of stimulated recovery to the dye ground state can be important and is delineated. This analysis of nonlinear absorption processes is applicable in general to situations where chromophores are irradiated, for instance, in biology. We examine the implications for the bending of cantilevers made of heavily dye-loaded nematic photosolids, that is nematic glasses and elastomers that have large mechanical reactions to light. In particular we describe the bending of cantilevers sufficiently absorbing that they would not bend if Beer's law were applicable. We quantify the role of optically generated heat in determining the mechanical response and conclude that in general it is minor in importance compared with optical effects.

DOI: 10.1103/PhysRevE.77.051710 PACS number(s): 61.30.Gd, 46.25.Hf, 46.70.De, 78.20.Hp

I. INTRODUCTION

Nematic solids are principally elastomeric [1] or glassy [2]. In each case they are composed of nematic polymers, but either loosely or tightly cross linked. Their moduli are accordingly low or high and they are capable of either huge or modest extensions. They form unique solids in that, when their order is changed, they can change their dimensions considerably and these mechanical responses can be steered in many ways. The order can either be redirected (director rotation under the influence of electric, mechanical or optical fields) or reduced. In this paper, for simplicity we concentrate on changing the magnitude of order, achievable by heating or cooling, or by the absorption of light into photoactive rods when they are a component of the nematic solid. The natural elongation of the oriented polymers making up the networks is modified by order change, with the result that macroscopic mechanical changes are induced. Reversible thermal strains of hundreds of percent have been observed in elastomers [3,4]. Smaller changes arise in glasses, where subtle arrangements of director have been employed to achieve more complex mechanical responses [2]. Since light and heat have analogous effects, one expects and indeed finds that optical absorption leads to analogous mechanical strains, both in photoelastomers [5,6] and in photoglasses [7]. Such a mechanism of mechanical change offers the possibility of micro-opto-mechanical **s**ystems (MOMS) where elements can be optically induced to bend as elastomeric photoswimmers [8] or as glassy cantilevers [7,9,10]. The bend arises because the contraction is differential with depth since the optical beam is absorbed and is hence weaker with depth. How the beam intensity varies with depth because of nonlinear absorption processes, and how this variation is translated into bending even in situations where absorption is so high that penetration would be negligible in the linear case, are the two questions that concern this paper. A schematic, Fig. 1, of the penetration and of the differential contraction leading to bend establishes the coordinate (x) of penetration, the thickness (w), and the curvature $(1/R)$ of the cantilever.

Light disrupts nematic order when molecular rods which are also chromophores, that is dye molecules, bend on absorbing a photon in their straight (*trans*) ground state and make an indirect transition to their bent (*cis*) excited state. The orientational order of tightly packed rods is thereby reduced by the *cis* fraction. We shall assume for simplicity that the mechanical contractile strain is proportional to the *cis* volume fraction. It is a vexed question as to whether heat released by these optically induced transitions is the actual cause of the order change. This question has been addressed by irradiating polydomain nematic photoglasses with polarized light. One finds [11] that the mechanical contraction occurs along the light polarization direction, a response that is therefore simply tunable by rotating the light polarization. Domains closely aligned to the optical electric field absorb, and thus also contract, preferentially over domains that are misaligned [12]. Moreover, since the domain size is small, heat diffusion is fast, and domains neighboring an absorbing region quickly reach similar temperatures. If temperature were the mechanism for contraction, it would thus under these conditions of fast diffusion not distinguish a preferred direction and there would be no overall effect (just as when one simply heats a polydomain nematic solid). Evidently, optical effects dominate. We discuss thermal effects at length in this paper and find their influence small, even across a whole monodomain cantilever, because of the diffusional rates that arise.

Since photons are absorbed by the dye components in the nematic, then light penetrating the face of a nematic photocantilever will be attenuated and hence the contractions generated diminish with depth. Curvature of the cantilever results, Fig. 1. It is important in micro-opto-mechanical **s**ystems (MOMS) where elements can be optically induced to bend as elastomeric photoswimmers [8] or as glassy cantilevers [9,10].

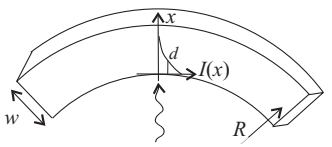

FIG. 1. Radiation penetration with linear absorption length d giving light-induced bend.

*mw141@cam.ac.uk

Weak beams decay exponentially with depth (Beer's law). The conversion of straight to bent (*trans*→*cis*) forms of the dye molecules is also exponential in this limit. For a linear connection (valid for small strains) between *cis* population and contraction, in the Beer limit maximum cantilever curvature is predicted [13] for $w/d \sim 2.63$, where w is the thickness of the cantilever and d is the exponential decay length: If $w \gg d$, only a thin skin of network contracts and its contractile stresses are insufficient to make the unstrained part of the cantilever below respond. Equally, if $w \ll d$, then there is little variation of photostrain through the thickness and the cantilever may contract but not differentially with depth and thus will bend little. The extent of bend, for a fixed w/d, was also predicted to be linear with intensity.

Experimentally, cantilevers are commonly heavily dye-doped but still show appreciable mechanical effects [14]. The above arguments suggest that this bending is unexpected: High dye concentrations mean strong absorption and hence small d. In this thin-skin limit, $d \ll w$, bend is expected to disappear. Evidently nonlinear effects lead to deep penetration of light and thus lead to bending. We shall explain these related effects by making two assumptions for simplicity to illustrate the underlying principles. We take the straightforward case of no photoinduced director rotation, that is for nematic glasses and constrained systems (for instance, where surface effects might be strong, where the director seems to be immobile under elongations imposed at an angle and also probably do not rotate during photoprocesses [15]. However, photoisomerization in glasses has additional subtleties; we derive the nonlinear penetration of intense beams into glass as well. Second, we assume that there is not appreciable reduction in the magnitude of the nematic order parameter under illumination. This assumption is reasonable in glasses, but in liquid and elastomeric nematics, this assumption is too restrictive. Indeed a description of polydomain nematic elastomer response invokes both order reduction and rotation [12]. We return elsewhere to the role order reduction and rotation play in nonlinear absorption and mechanics.

An initial attack on this problem [16] invoked photobleaching, that is depletion of the *trans* form, letting light through to greater depths than would be expected by Beer's law. Here we derive these nonlinear effects fully, paying attention to two additional influences that are potentially important. The optically stimulated back reaction *cis*→*trans* can alter the nonlinear processes considerably and is of importance when the *cis* absorption line is not widely separated from that of the *trans* species. Second, thermal effects could be considerable, all the more so because of a possibly nearby nematic to isotropic transition where giant thermomechanical effects are known to occur, especially in elastomers.

The remainder of this paper is organized as follows. In Sec. II we derive equations which describe the attenuation of light passing through a region with photoactive chromophores. Our analysis of nonlinear absorption is thus relevant to a wide range of situations where dye is irradiated, and is not limited to mechanics, which is our ultimate aim here. Our methods and results are similar to a penetrating analysis, experimental and theoretical, of Statman and Janossy [17]. In Sec. IV we show how optical attenuation leads to cantilever bending and calculate the radius of curvature as a function of the incident flux of light. In Sec. V we investigate the distribution of strain throughout the bent sample, and in particular we demonstrate that there can be several planes within the cantilever on which the net strain is zero. In Sec. VI we discuss the possible effects of temperature change owing to absorption of photons on the results presented thus far. We find that, for intense illumination, temperature distributions are symmetric about the cantilever mid-plane and hence do not contribute to bend, only contraction. Finally in Sec. VII we present our conclusions.

II. ATTENUATION

We consider the situation of Fig. 1(b) of a long, slender cantilever of thickness w illuminated by light with incident flux I_0. The absolute number density of chromophores is ρ_{ph}. At a time t after the onset of illumination and depth x within the cantilever, the fraction of these chromophores in the straight *trans* state is $n_t(x,t)$ and the fraction in the bent *cis* state is $n_c(x,t)=1-n_t(x,t)$. The magnitude of the Poynting flux at x and t is $I(x,t)$. The dynamics of the *trans* fraction is determined by three processes, (i) an optically stimulated *trans*→*cis* reaction with rate $\Gamma_1 I(x,t) n_t(x,t)$, (ii) an optically stimulated *cis*→*trans* back reaction with rate $\Gamma_2 I(x,t) n_c(x,t)$, and (iii) a spontaneous, thermally activated, *cis*→*trans* back reaction with characteristic time τ. Γ_t and Γ_c subsume absorption cross sections per chromophore and the quantum efficiencies Φ_{tc} and Φ_{ct} of the stimulated *trans-cis* reaction and *cis-trans* back reaction, respectively, see [17] for the rate equations in full with such factors explicitly given. We take the absorption cross sections to be independent of nematic order—as discussed above, changing nematic order is itself another source of nonlinearity. Combining these three rates we obtain for the rate of change of the *trans* fraction

$$\frac{\partial n_t}{\partial t} = -\Gamma_t I(x,t) n_t(x,t) + \left(\frac{1}{\tau} + \Gamma_c I(x,t)\right) n_c(x,t). \qquad (1)$$

In this paper we confine ourselves to the steady state, that is $\frac{\partial n_t}{\partial t}=0$. Setting this condition in Eq. (1) and taking out a factor of τ gives the steady state *trans* and *cis* populations,

$$n_t(x) = \frac{1+\Gamma_c \tau I}{1+(\Gamma_t+\Gamma_c)\tau I}, \quad n_c(x) = \frac{\Gamma_t \tau I}{1+(\Gamma_t+\Gamma_c)\tau I}, \qquad (2)$$

where I is now $I(x)$ simply, and will be determined below. We can identify two characteristic, material intensities, $I_t = 1/(\Gamma_t \tau)$ and $I_c = 1/(\Gamma_c \tau)$. It is convenient to scale the flux by its incident value, thus $\mathcal{I}(x,t)=I(x,t)/I_0$. The reduced intensity is thus $\mathcal{I}=1$ at the entry surface $x=0$, see Fig. 1(b). We also define dimensionless quantities $\alpha = I_0/I_t$ and $\beta = I_0/I_c$. These are the incident flux reduced by fluxes I_t or I_c characteristic of *trans* or *cis* molecules, respectively. We refer to α and β subsequently as reduced incident fluxes. Ignoring for the moment attenuation, α measures how much a beam intensity I_0 leads to *trans* conversion, Eq. (1), by comparing I_0 to I_t, that is the ratio of the forward rate to the thermal backward rate, $\alpha = I_0/I_t = I_0 \Gamma_t/(1/\tau)$. Likewise, β is the ratio of the induced to the thermal back rates.

In terms of the reduced incident intensities α and β, the steady-state *trans* and *cis* populations are given by

$$n_t(x) = \frac{1+\beta\mathcal{I}}{1+(\alpha+\beta)\mathcal{I}}, \quad n_c(x) = \frac{\alpha\mathcal{I}}{1+(\alpha+\beta)\mathcal{I}}. \tag{3}$$

Here $\mathcal{I}$ is just $\mathcal{I}(x)$ since we have the equilibrium case. In the Eisenbach experiments [18] the average conversion was $n_c \sim 0.84$. His measurements of attenuation suggested $\beta \sim 0$, and thus one can conclude from Eq. (3) that his $\alpha \sim 5$. Note that α and β are independent of chromophore concentration, but do depend on the choice of the light polarization [17]. Experimentally it is easiest to determine α for a system dilute in chromophores, where one can ignore the complications arising when attenuation is significant. These estimates for α are lower bounds on actual values; including the effects of attenuation through the cantilever will lead to higher values of α. In later work [5] one can deduce that $\alpha \sim 0.8$.

The divergence of the Poynting flux, $\frac{\partial I}{\partial x}$, at any point through the cantilever is equal to the amount of energy taken out of the beam per unit volume per unit time. For simplicity, we ignore curvature leading to obliquity factors for the intensity of light falling on the surface. That is, we consider small deflections or diffuse light. Energy is taken out of the beam both by the optically induced *trans*$\rightarrow$*cis* reaction and by the stimulated *cis*$\rightarrow$*trans* back-reaction, terms (i) and (ii) above. The divergence of the Poynting flux is thus related to the sum of the rates of these two processes. Thus,

$$\frac{\partial I}{\partial x} = -\gamma_t\Gamma_t I(x,t)n_t(x,t) - \gamma_c\Gamma_c I(x,t)n_c(x,t), \tag{4}$$

where the constant γ in each case subsumes the energy of an incident photon, $\hbar\omega$, the reciprocal of the quantum efficiency Φ for the relevant transition, and the absolute number density of chromophores, ρ_{ph} (which could differ between *trans* and *cis* forms since bent molecules pack less efficiently). The appearance of Φ as an inverse is required since for each successful transition in the rate $\Gamma_i I n_i$ (i=t,c) there will be unsuccessful absorptions that do not contribute to $\partial n_t/\partial t$ in (1), but nevertheless still deplete the optical beam and contribute to $\partial I/\partial x$ in (4).

Equations (1) and (4) are a pair of coupled, nonlinear, first-order partial differential equations for $I(x,t)$ and $n_t(x,t)$. Solving these equations subject to the boundary conditions $I(0,t)=I_0$ and $n_t(x,0)=1$ is in general complex, though analytically possible in some limits. We return to this problem elsewhere [19] and here take the time-independent, equilibrium state. Thus, using $n_c=1-n_t$, dividing through by the incident intensity I_0, and letting $d_t=1/(\gamma_t\Gamma_t)$ and $d_c=1/(\gamma_c\Gamma_c)$ denote the characteristic lengths for optical attenuation by *trans* and *cis* chromophores, respectively, one obtains [16,17]

$$\frac{d\mathcal{I}}{dx} = -\left[\left(\frac{1}{d_t} - \frac{1}{d_c}n_t + \frac{1}{d_c}\right)\right]\mathcal{I}(x). \tag{5}$$

In terms of the parameters α and β, the ratio of the *trans* and *cis* lengths is $d_t/d_c=(\gamma_c/\gamma_t)(\beta/\alpha)$. The ratio $\eta=\gamma_c/\gamma_t$ is the ratio of the quantum efficiencies for the *trans*$\rightarrow$*cis* and *cis*$\rightarrow$*trans* reactions, that is $\eta=\Phi_{tc}/\Phi_{ct}$. We shall take $\eta=1$ in the numerical illustrations in this paper. We have ignored any attenuation by the host material; one could include such effects by adding a simple Lambert-Beer term $-I(x,t)/d_h$ to the right-hand side of Eq. (4) or Eq. (5). See Sec. III A for an analysis.

Inserting the steady-state expression for n_t from Eq. (3) into Eq. (5), and then integrating with respect to x, subject to $\mathcal{I}(x=0)=1$, we obtain (see also [17])

$$\ln\mathcal{I} + \left(\frac{\alpha-\eta\beta}{\beta'}\right)\ln\left(\frac{1+\beta'\mathcal{I}}{1+\beta'}\right) = -\frac{x}{d_t}, \tag{6}$$

where $\beta'=\beta(1+\eta)$. In general this expression is very different from Beer's law, $\mathcal{I}(x)=\exp(-x/d)$.

Deviations from Beer's law come about because at high intensities the *cis* population increases (bleaching) and is generally less absorbing than the *trans* species. Optical penetration is then more effective and is of great significance for photomechanics. To most simply see how nonlinearities (bleaching) manifest themselves, consider the limit $\beta\rightarrow 0$ [16] that arises when stimulated *cis* back conversion is weak (for instance, in the work of Eisenbach). Under those circumstances $\Gamma_c \sim 0$ in Eq. (1), and then (5) takes the form

$$\frac{d\mathcal{I}}{dx} = -\frac{n_t}{d_t}\mathcal{I}(x). \tag{7}$$

A non-Beer form arises because $n_t=1/(1+\alpha\mathcal{I})$ itself depends on $\mathcal{I}$, Eq. (3). Integration gives

$$\ln\mathcal{I} + \alpha(\mathcal{I}-1) = -x/d_t, \tag{8}$$

also a $\beta\rightarrow 0$ limit of (6), equivalent to Eq. (18) in [20]. A formal solution of which is $\mathcal{I}(x)=\frac{1}{\alpha}W_L(\alpha e^{\alpha-(x/d_t)})$, where $W_L(x)$ is the Lambert-W function [21]. The nonexponential decay persists until around $\alpha\mathcal{I}<1$, whereupon n_t becomes independent of $\mathcal{I}$ and (7) reverts to simple exponential form.

The limiting cases of absorption are important.

(i) $(\alpha+\beta)\mathcal{I}\ll 1$. Now $n_t\approx 1$ and $n_c\approx 0$ which renders (5) trivially of the Beer form. The limit is obtained when $\alpha=I_0/I_t$ and $\beta=I_0/I_c$ are both $\ll 1$ (since $\mathcal{I}$ is bounded by 1), that is, the incident beam is weak compared with both material fluxes I_t and I_c. It is also obtained when α and β are not small, but when $\mathcal{I}\ll 1/(\alpha+\beta)$, that is when the beam has diminished (albeit linearly rather than exponentially, see the sketch below and also the high intensity traces of Fig. 2) to the point that $n_t=\text{const}\approx 1$ and Beer behavior is finally recovered. From (8) one sees in fact $\mathcal{I}(x)\sim\exp[-(x-d_t\alpha)/d_t]$ for $x>d_t\alpha$, a shifted Beer form. Exponential decay is the ultimate fate of all optical beams provided that cantilevers are thick enough to get this diminution of intensity.

(ii) The high flux limit $\alpha\mathcal{I}\gg 1$ (with $\beta\sim 0$) is where the forward reaction dominates over thermal back reaction. Photoequilibrium is highly biased away from *trans*, that is in Eq. (3) $n_t\sim 1/(\alpha\mathcal{I})$. Equation (7) reduces to $\mathcal{I}'\sim -1/(\alpha d_t)$, whence $\mathcal{I}\sim 1-x/(\alpha d_t)$. This linear penetration for $x\lesssim\alpha d_t$ is evident in Fig. 2 at the higher α values and is at the heart of why even highly absorbing systems can be responsive. When $x\gtrsim\alpha d_t$, decay is again exponential, see above.

(iii) The high flux limit, $\beta\mathcal{I}\gg 1$, that is $I\Gamma_c\gg 1/\tau$, is where the stimulated back reaction dominates over the thermal back

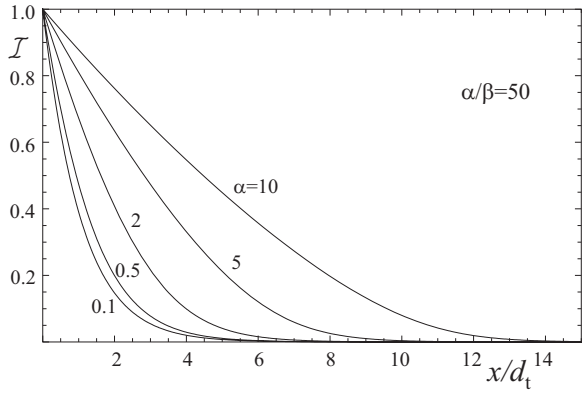

FIG. 2. The decay in reduced light intensity with reduced depth for various reduced incident intensities α, with a weakly stimulated back reaction such that $\alpha/\beta=50$. The plots are similar to those for $\beta=0$, with small differences we discuss when considering heat generation.

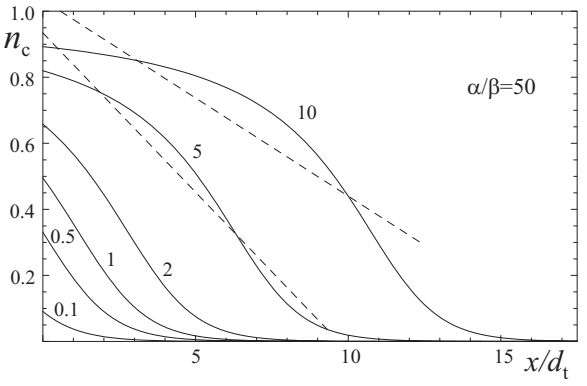

FIG. 3. The decay in *cis* number fraction $n_c(x)$ with reduced depth for various reduced incident intensities α, with $\alpha/\beta=50$. Increasing α extends the conversion to *cis* to greater depths because of photobleaching of the surface layers. Reduced geometric bend strain for $\alpha=5$, 10 are shown as straight dotted lines. For cantilevers of thickness $w=w*=9.313d$ and $w=12.5d$, respectively, there are three and two intersections (neutral surfaces) with the photostrain curves.

reaction. In that case $n_t \to \beta/(\alpha+\beta)$ and $n_c \to \alpha/(\alpha+\beta)$ are again constants and again (4) takes a Beer form in the equilibrium limit,

$$d\mathcal{I}/dx = -\mathcal{I}\beta(1+\eta)/[d_t(\alpha+\beta)]. \tag{9}$$

The decay is exponential, $\mathcal{I}=\exp(-x/d_{\text{eff}})$ with an effective decay length $d_{\text{eff}}=d_t(\alpha+\beta)/[\beta(1+\eta)]$.

Thus, except for $\beta \ll 1$, profiles start in a Beer manner, have an intermediate nonexponential behavior if we have $\alpha > 1$ with $\beta \ll \alpha$, and then conclude with another Beer decay. The intermediate regime, $\beta\mathcal{I} \sim 1$, is where the stimulated back-reaction rate is comparable to the thermal rate.

(iv) When the decay lengths accidentally coincide, $d_t = d_c = d$, that is $\gamma_t\Gamma_t = \gamma_c\Gamma_c$, one can easily see in either (4) or in (5) that a Beer form pertains at all intensities or depths into the photoisomerizing medium, $\mathcal{I}=\exp(-x/d)$.

Statman and Janossy [17] investigated photoisomerization of solutions of the commercially available azodye Disperse Orange (DO3). They obtained a ratio of $\alpha/\beta \sim 5$ while the accessible range of α is up to ~ 80 (corresponding to an incident flux of 15 mW/mm^2). The spectral bands for *trans* $\to$ *cis* and *cis* $\to$ *trans* overlap quite strongly for DO3; one might thus expect much smaller ratios of β/α to be accessible when using dyes with more separated absorption bands. Indeed, Eisenbach's attenuation study showed that, for his systems, $d_c \gg d_t$ and thus that $\alpha \gg \beta$, possibly $\alpha \sim 100 \times \beta$. We thus show results initially for high ratios α/β for a range of incident intensities α and then look at smaller ratios where the nonlinear region is not so pronounced.

As can be seen from Eq. (3), the *cis* population is always reduced when β is finite. Thus for nonzero β we require a larger value of α to achieve a particular value of n_c. Similarly attenuation will lead to reduced intensities lower than unity in Eq. (3), again requiring larger values of α to achieve the same *cis* concentration. Thus estimates of α from absorption are lower bounds on true values.

A. Case 1—$\alpha/\beta=\infty$

We recall the case in which the illuminating light does not excite the *cis* $\to$ *trans* back reaction at all, i.e., $\beta=0$. Thus the intensity is described by Eq. (8). Plots are given in [16], but Fig. 2 for the case $\alpha/\beta=50$ of relatively small β also shows how for low α the decay from the surface intensity is exponential, but that penetration is much deeper for higher α, being initially a linear decay until finally decaying as an off-set exponential beyond the characteristic depth d_t, that is for $x > d_t\alpha$.

Such nonexponential behavior suggests caution when trying to establish an extinction length from the attenuation of a light beam on traversing a cantilever. For instance [14], an attenuation of 99% on traversing a cantilever of thickness 1 μm, where Beer's law is being followed, would result from an extinction length of $d_{\text{Beer}}=1\ \mu\text{m}/[2\ \ln(10)] \sim 0.22\ \mu$m. But if α is not small, much more light penetrates to $x=w$ (Fig. 2 is a guide). The d_{Beer} value derived is a gross over-estimate of d_t. Solving for d_t from Eq. (8) for a given attenuation $\mathcal{I}(w)$ on reaching the back face at $x=w$ yields for 99% attenuation, $d \sim w/(\alpha+4.6)=1\ \mu\text{m}/(\alpha+4.6) \to 0.04\ \mu$m for $\alpha=20$. The true d_t associated with a possible exponential decay may thus be much lower than the value d_{Beer} estimated as above, an indication that light has penetrated much further into the sample than would be expected for a simple exponential profile. Quantitative measurements of light attenuation varying with thickness or varying with incident intensity would resolve this ambiguity about d_t and also allow a determination of α. Attenuation at one thickness can only give an upper bound on d_t.

The reasons for departures from Beer's law for the intensity can be seen by returning the solution $\mathcal{I}(x)$ to Eq. (3) to obtain the spatial variation of the *cis* concentration. Figure 3 for the case $\alpha/\beta=50$ is a guide to the $\beta=0$ plots (see [16]) and displays exponential decay in $n_c(x)$ following $\mathcal{I}(x)$ for low intensity ($\alpha=0.1, 0.5$). High incident intensity not only lifts $n_c(x=0)$ at the surface, but also flattens the decay with depth—high n_c means low $n_t=1-n_c$ and hence fewer *trans* dye molecules in a state to deplete the incoming beam (a photobleached state). With photobleached surface layers, radiation penetrates well beyond $x \sim d_t$, and equally, contrac-

tion extends deep into the bulk, certainly beyond the Beer penetration depth d_t.

For $\alpha=0.5$ a point of inflection first appears at the surface, and moves inwards with increasing incident intensity α. The *cis* fraction at the inflection is always $n_c=1/3$ in this model. In the general case where $\beta\neq 0$ we find that the value of α at which the point of inflection first appears at the front surface is a complicated function of the constant ratio β/α, and the value of the *cis* fraction at the inflection point is no longer 1/3. From Eq. (3), the surface *cis* concentration is $n_c(0)=\alpha/(1+\alpha)$, since there $\mathcal{I}=1$, and rises to saturation, $n_c=1$, as intensity increases. The precise form of the cantilever bend depends critically on the shape of these $n_c(x)$ curves. In particular the development of a point of inflection allows three intercepts of the straight, geometric strain curves, and thus three neutral surfaces, we will later see. Since $n_c(x)$ changes shape with increasing intensity, we will find an elastic response that is highly nonlinear with intensity.

B. Case 2—$\alpha/\beta=50$

We now consider the case with a weakly stimulated back reaction, $\beta=\alpha/50$, and henceforth take $\eta=1$. Figure 2 shows plots of the reduced intensity as a function of x/d_t. The reduced intensity curves are largely identical to the $\beta=0$ case. Once again, for small values of α (=0.1,0.5) the decay is essentially exponential, with a characteristic length given by d_t. Increasing α leads to deeper penetration, with the initial decay being essentially linear. However, close inspection of the $\alpha=10$ curve reveals a slight upwards curvature, a result of the higher-order corrections in β that take us from (8) to (6). Eventually $\mathcal{I}(x)$ becomes exponential at penetration depths $x\sim d_t\alpha$ significantly greater than d_t.

As we show above, for $\beta\gtrsim 1$, that is here $\alpha\gtrsim 50$, the initial behavior should (briefly) revert to being exponential before attaining the linear decay associated with non-Beer. This point is easier to display below when we consider smaller α/β ratios.

The *cis* profiles as a function of depth are shown in Fig. 3. For the values of α plotted, the curves are essentially identical to those in the $\beta=0$ case. High incident intensities result in larger *cis* fractions near the surface, and a flatter decay as before. The point of inflection occurs for a *cis* fraction less than the 1/3 found in the $\beta=0$ case, but it is still of importance that inflections exist for the character and number of neutral surfaces we explore later.

C. Case 3—$\alpha/\beta=5$

Increasing the stimulated back reaction further we take $\alpha/\beta=5$. The curves for the reduced intensity as a function of depth, see Fig. 4, now differ somewhat from those in the small β limit, e.g., as in Fig. 2. For the smaller values of α the curves remain exponential with a characteristic length d_t. Increasing α leads to some increased penetration, without showing the long linear decay in reduced intensity seen in Fig. 2. For $\alpha=10$ we have $\beta\mathcal{I}=2$ at most, a value evidently insufficient to satisfy limit (iii). We do not have a finite initial region for small x where the decay is exponential with d_{eff} given in and below Eq. (9). For these values of α and β one would have $d_{\text{eff}}=3d_t$. The dashed line shows the infinite α limit, and corresponds throughout its range to Eq. (9), i.e., an exponential with characteristic length $d_{\text{eff}}=d_t(\alpha+\beta)/[\beta(1+\eta)]=3d_t$. Note that the initial slope of the $\alpha=10$ curve is close to that of the $\alpha=\infty$ curve.

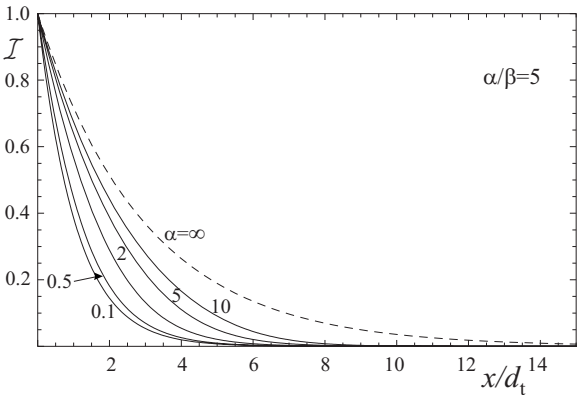

FIG. 4. The decay in reduced light intensity with reduced depth for various reduced incident intensities α with $\alpha/\beta=5$.

The corresponding *cis* profiles as a function of depth are shown in Fig. 5. In comparison with Fig. 3 we see that the *cis* population at the surface is lower in the present case, and that the decay of the *cis* population with depth is more rapid.

III. OTHER ABSORPTION PROCESSES

At least two other influences are important in nonlinear absorption. How does one deal with the absorption of the host material that is not a chromophore. In principle this is the simplest form of absorption and for weak beams where both processes are Beer-like the effect can simply be divided out. We examine how this procedure translates to the nonlinear case. Another, more complex effect is that of the host medium when it is a solid. The isomerization processes can be biased by mechanical effects, as is well known from linear experiments. These influence the nonlinear absorption for intense beams.

A. Beer-Lambert host absorption

It will always be the case that the host for the chromophores will also absorb light. For simplicity ignoring the

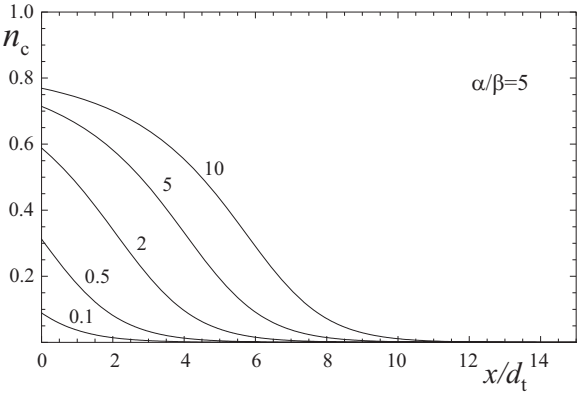

FIG. 5. The decay in *cis* number fraction $n_c(x)$ with reduced depth for various reduced incident intensities α with $\alpha/\beta=5$.

back reaction, $\beta=0$, the absorption equation (5) becomes

$$\frac{d\mathcal{I}}{dx} = -\left(\frac{n_t}{d_t} + \frac{1}{d_h}\right)\mathcal{I}(x). \tag{10}$$

The absorption length d_t of course emerges naturally by measuring the absorption of a sample without dye, $-\ln(\mathcal{I}_w) = w/d_h$. Using $n_t = 1/(1+\alpha\mathcal{I})$, and denoting the ratio of absorption lengths $\psi = d_t/d_h$, integration yields

$$\ln(\mathcal{I}_w) + \frac{1}{\psi}\ln\left(\frac{1+\psi(1+\alpha\mathcal{I}_w)}{1+\psi(1+\alpha)}\right) = -w/d_{\text{eff}}, \tag{11}$$

where the effective absorption length is $1/d_{\text{eff}} = 1/d_t + 1/d_h$. The relation (11) for $\mathcal{I}_w$ has close similarities to that for the profile with a back reaction, Eq. (6). The limit $\psi \to 0$ of Eq. (11) of no host absorption leads to the previous Lambert-W expression given below Eq. (8). In the conclusions we discuss how host absorption can be allowed for in measurements.

B. Absorption of intense beams in solid hosts

The role of the host has been much studied in dynamical studies of absorption. When the host, typically a polymer or a network, is below the glass temperature then it is observed that there is more than one characteristic decay time for the *cis* population of guest chromophores. Eisenbach [22] clearly observed 2 times the relative weight of the processes being dependent upon temperature. The slower process was analogous to that observed in a liquid host and becomes the only process present at elevated temperatures. The faster process was speculated to arise from the strained state of a *cis* isomer; a fraction of the molecules when in a bent state are in conflict with the solid matrix around them and thereby decay more quickly to the *trans* form. Other authors [23] suggest that there is a spectrum of relaxation times corresponding to a range of environments that *cis* chromophores find themselves in. Eisenbach also found that, when above its glass temperature, rubber provides a liquidlike environment for its chromophore guests. There was only one relaxation time and this was comparable to that found when chromophores were dissolved in liquids, a fact of considerable importance since elastomers are used as photomechanical media.

Ignoring for simplicity photoinduced back reactions (as shown to be the case, for instance, in the Eisenbach study), the dynamical equation (1) is modified in that in principle the forward rate Γ_t could become a function of environment (denoted by p) and the thermal back-reaction rate $1/\tau$ is certainly a function of p. The result is that the characteristic reduced intensity is now a function of environment and we denote it by $\alpha_p = \Gamma_{tp}\tau_p I_0$. The equilibrium *trans* number fraction for chromophores in the environment p is thus $n_{tp} = 1/(1+\alpha_p\mathcal{I})$, see Eq. (3). Let the probabilities of finding a chromophore in the p environment be a_p. Then the total *trans* volume fraction of chromophores is $n_t = \Sigma_p a_p/(1+\alpha_p\mathcal{I})$, and it is this n_t that must appear in Eq. (4),

$$\frac{1}{\mathcal{I}}\frac{d\mathcal{I}}{dx} = -\frac{1}{d_t}\sum_p \frac{a_p}{1+\alpha_p\mathcal{I}}, \tag{12}$$

$$-\frac{w}{d_t} = \int_1^{\mathcal{I}} \frac{d\mathcal{I}}{\mathcal{I}\left(\dfrac{a}{1+\alpha_1\mathcal{I}} + \dfrac{1-a}{1+\alpha_2\mathcal{I}}\right)}, \tag{13}$$

$$-\frac{w}{d_t} = \frac{1}{\alpha}\left(\alpha_1+\alpha_2-\alpha-\frac{\alpha_1\alpha_2}{\alpha}\right)\ln\left(\frac{1+\alpha\mathcal{I}}{1+\alpha}\right) + \ln(\mathcal{I}) - (1-\mathcal{I})\frac{\alpha_1\alpha_2}{\alpha}. \tag{14}$$

The first equation is general, the second two have been specialized to the Eisenbach case of two decay rates and thus α_1 and α_2 with weights a and $1-a$, respectively. Here $\alpha = a\alpha_1 + (1-a)\alpha_2$; note that this is not an averaged α_p. Again, this result has similarities of form with the $\beta \neq 0$ form (6) and the host absorption result (11), and is derived by the same kinds of integrations.

IV. OPTICALLY INDUCED CURVATURE

Figure 1 shows a cantilever with radius of curvature R. The geometric strain from bending is $x/R+K$, where R is the radius of curvature adopted by the cantilever and K is a mean strain, both to be determined for a given thickness w and illumination. Illumination changes the natural length of the sample, the actual strain with respect to this new natural length is $x/R+K-\epsilon_p = x/R+K+An_c(x)$ which, if we further reduce x/R and K by the dimensionless constant A connecting photostrain ϵ_p and the *cis* concentration, we obtain $x/R+K+n_c(x)$ for the effective reduced strain. A linear relation between *cis* concentration and strain is probably valid for nematic glasses, but for elastomers it is possible to reach the isotropic state by illumination at temperatures close enough to the nematic-isotropic transition and the relation is no longer linear, but can be mapped onto the observed variation of strain with temperature [5]. The mechanical stress σ is related linearly to the strain via the Young's modulus E. Since there are no external forces nor external torques, mechanical equilibrium requires vanishing total force and moment across a section, thus

$$\int_0^w \sigma(x)dx = E\int_0^w \left(\frac{x}{R}+K+n_c(x)\right)dx = 0,$$

$$\int_0^w x\sigma(x)dx = E\int_0^w x\left(\frac{x}{R}+K+n_c(x)\right)dx = 0. \tag{15}$$

When the modulus is constant it drops out, but must generally be retained (for some photoglasses E is known to vary with illumination [15]). Performing these integrations we have

$$\frac{w^2}{2R} + Kw = -\int_0^w n_c(x)dx, \tag{16}$$

$$\frac{w^3}{3R} + \frac{Kw^2}{2} = -\int_0^w x n_c(x) dx. \tag{17}$$

Simplifying between these two expression we obtain for the radius of curvature

$$\frac{1}{R} = \frac{12}{w^3}\int_0^w \left(\frac{w}{2} - x\right) n_c(x) dx. \tag{18}$$

Equation (5) can be rearranged to give an expression for $n_c(x)$, recalling $d_t/d_c = \eta\beta/\alpha$, $\eta = \gamma_c/\gamma_t$, and $n_t = 1 - n_c$,

$$n_c(x) = \frac{1}{1 - \eta\dfrac{\beta}{\alpha}} + \frac{d_t}{1 - \eta\dfrac{\beta}{\alpha}} \frac{1}{\mathcal{I}} \frac{d\mathcal{I}}{dx}. \tag{19}$$

Inserting this expression into Eq. (18) and changing integration variables $\int_0^w dx \to \int_{\mathcal{I}_0=1}^{\mathcal{I}_w} d\mathcal{I}$, we have

$$\frac{d_t}{R} = 12\left(\frac{d_t}{w}\right)^3 \frac{1}{1 - \eta\dfrac{\beta}{\alpha}} \int_1^{\mathcal{I}_w} \left(\frac{w}{2d_t} - \frac{x}{d_t}\right) \frac{d\mathcal{I}}{\mathcal{I}}. \tag{20}$$

Substituting for x/d_t and w/d_t from Eq. (6) and integrating, we obtain [with $\beta' = \beta(1+\eta)$]

$$\frac{d_t}{R} = \frac{12\alpha}{\beta'(w/d_t)^3}\left(\mathrm{Li}_2(-\beta') - \mathrm{Li}_2(-\beta'\mathcal{I}_w) - \frac{1}{2}\ln(\mathcal{I}_w)\ln[(1+\beta'\mathcal{I}_w)(1+\beta')]\right), \tag{21}$$

where $\mathrm{Li}_2(x) = \int_x^0 dt \frac{\ln(1-t)}{t} = \Sigma_{k=1}^{\infty} \frac{x^k}{k^2}$ is the dilogarithm [24]. The limit $\beta \to 0$ within this expression recovers our earlier expression for the curvature [16],

$$\frac{d_t}{R} = \frac{12\alpha d_t^3}{w^3}\left[\frac{w}{d_t}\mathcal{I}_w - (1-\mathcal{I}_w)\left(1 - \frac{w}{2d_t}\right) - \frac{\alpha}{2}(1-\mathcal{I}_w^2)\right]. \tag{22}$$

At low incident light intensity, $\alpha \to 0$, analysis [13] for exponential decay gave maximal reduced curvature $w/\alpha R$ for $w/d \sim 2.63$. In this limit $1/R \sim \alpha \sim I_o$, hence the division by α to obtain results universal for all (low) intensities of incident light. As intensity increases, the maximum in $w/\alpha R$ moves to larger w/d because the radiation penetrates more deeply.

The nonlinear regime, at fixed Beer's law penetration d_t, is best revealed by reducing R by d_t instead of by w, and by not reducing $1/R$ by α. Figure 6 plots d_t/R against w/d_t to reveal maxima in d/R at greater w as intensity α and thus penetration increases. At a given w/d_t, one sees curvature increase initially with intensity, the Beer limit, and then reduce as penetration increases and gradients of strain are reduced. Thus appreciable curvature arises experimentally even in cantilevers thick in the sense $w \gg d_t$: In [11] it appears that curvature is induced even though the cantilevers involved (with $w = 10$ μm) are apparently at least 100 times thicker than their extinction length (see also [14]). The curvatures against thickness for various intensities α in the case of $\alpha/\beta = 50$ studied above are practically identical to those in the $\beta = 0$ limit of [16]. As the back-reaction rate increases relative to the forward rate, $\alpha/\beta = 5$, the penetration is less and the curvature maxima move to noticeably smaller reduced thicknesses w/d_t, see lower pane.

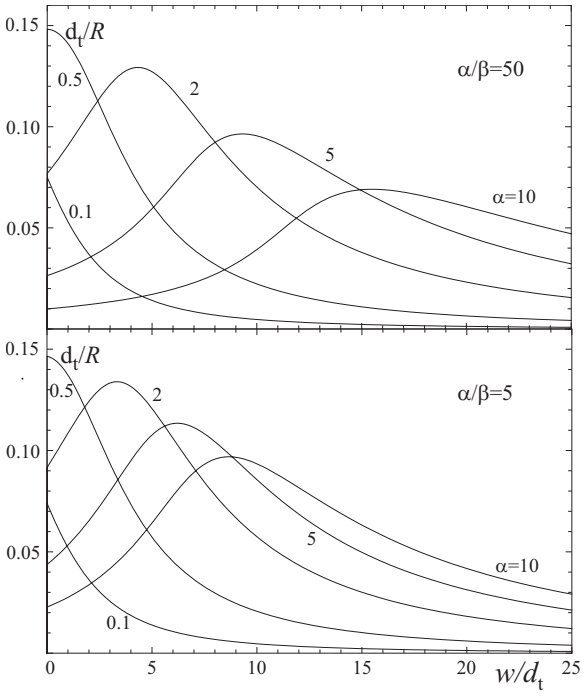

FIG. 6. Curvature reduced by $1/d_t$ against reduced cantilever thickness w/d_t for various incident reduced light intensities α, with $\alpha/\beta = 50$ (upper) and =5 (lower). For high intensities, bleached surface layers let light penetrate more deeply and hence a significant fraction of the cantilever has its natural length contracted. Bend occurs even for cantilevers much thicker than the linear penetration depth d_t. Maxima in curvature occur at smaller thicknesses than in the $\beta = 0$ case where back reaction is purely thermal, and are seen at ever smaller thickness as β increases.

In the limit of intense illumination, that is $\alpha \gg 1$, the intensity profile simplified to $\mathcal{I} \simeq 1 - x/(\alpha d_t)$ for penetration $x < \alpha d_t$ and hence intensity such that $\alpha\mathcal{I} > 1$. Under these circumstances $n_c \simeq 1 - 1/(\alpha\mathcal{I})^2$ and, importantly for the curvature, $n_c' \simeq -1/[d_t(\alpha\mathcal{I})^2]$. If the thickness $w \ll \alpha d_t$, then the largely linear profile of $\mathcal{I}(x)$ is obtained through most of the thickness of the cantilever and also $\mathcal{I} \sim 1$. One can then approximate $n_c' \simeq -1/(d_t\alpha^2)$. While the strain follows $n_c(x)$ linearly, then there will be a linear change of photostrain, that is new natural state of the cantilever, through the thickness. If the geometric bend follows this exactly, then there is no effective internal stresses in the material. This condition fixes the curvature as $d_t/R = A/\alpha^2$. We thus see that this definition of very strong irradiation involves the thickness w in relation to αd_t. It is a condition that penetration is so deep that light emerges from the other side of a heavily dye-loaded sample since there is no region of exponential decay of $\mathcal{I}(x)$. Moreover, because of the deep penetration, the curvature now diminishes with increasing intensity (such as $1/\alpha^2$), rather than increasing. The time taken for the profile to reach the highly bleached form above can be long, a problem we return to in modeling the nonlinear dynamics of intense absorption [19].

Quantitative measurements of reduced curvature w/R with I_o are required to probe this complex dependence of curvature on thickness and incident intensity. Particular care must be taken to irradiate long enough for equilibrium to be reached, and possibly curvature to reduce from high intermediate values.

V. STRAIN DISTRIBUTIONS

In the linear case [13] of bend induced by exponentially decaying optical intensity, two neutral surfaces arise, that is surfaces of zero stress where the geometric strains arising from curvature happen to match the local photostrain, $x_n/R+K+n_c(x_n)=0$. A classical cantilever bent by imposed terminal torques has a single neutral surface at its midpoint $x_n=w/2$, so that stresses that are equal and opposite about the $x=w/2$ sum to zero to give no net force. In the current case of cantilevers bending because of strains generated internally by light, rather than by external imposition of torques, the additional constraint of no net torque leads to a more complex distribution of stresses which gives rise to more than one neutral surface.

The maximum values for both the curvature $1/R$ and contraction K are intimately related to the positions of the neutral surfaces. Differentiating Eqs. (16) and (17) with respect to the cantilever thickness w and solving between the resulting equations, we obtain the relationship

$$\frac{dR}{dw}=\frac{3R^2}{w}\frac{dK}{dw}, \tag{23}$$

thus both $1/R$ and K are maximized for the same cantilever thickness. Furthermore, returning $dR/dw=dK/dw=0$ to either of the differentiated equations, one finds that the thickness at which this happens, w^*, satisfies $w^*/R+K+n_c(w^*)=0$, i.e., the straight line of geometrically induced strain intersects the photostrain $[\sim n_c(x)]$ curve at the back surface of the cantilever. The back surface is a neutral surface when the curvature is maximized. The curve $n_c(x)$ is always a strictly decreasing function of x; however there is a fundamental difference between the curves in the $\beta=0$ case for $\alpha<0.5$ and those for $\alpha>0.5$—the latter $n_c(x)$ curves have a point of inflection $[n_c''(x)=0]$. The straight line of geometrically generated strain imposed from curvature, $-(x/R+K)$, can intersect the $n_c(x)$ curve at most two times if there is no point of inflection, and at most three times if there is a single point of inflection. It is not possible for the strain to satisfy the constraints of vanishing force and torque, that is to satisfy Eqs. (15), and have a neutral surface at the back surface of the beam with only two neutral surfaces; thus there is no maximum for the curvature unless the underlying *cis* curve has an inflection point. For $\beta\neq 0$ the α value that divides the curves into those with and those without an inflection point is no longer exactly $\alpha=0.5$ but, as can be seen in Fig. 3, for small β the division is still at an α close to 0.5.

To illustrate the significance of inflections, two sample curvature strains of purely geometric origin are superimposed in Fig. 3. On the $\alpha=10$, $\beta=0.2$ curve is also plotted the straight line $-(x/R+K)$ for a cantilever of thickness $w=12.5d_t$, a thickness that is before the inflection point in the $n_c(x)$ curve. As can be seen, the straight line intersects the underlying $n_c(x)$ curve only two times in satisfying Eqs. (15) and locates only two neutral surfaces. On the $\alpha=5$, $\beta=0.1$ curve is also plotted $-(x/R+K)$ for the critical thickness $w=w^*=9.313d_t$ where the third neutral surface first appears. One sees that this line intersects the underlying $n_c(x)$ curve three times, internally two times with the third intersection (neutral surface) coinciding with the back surface. This line is that of maximal possible slope, $dR/dw=0$. With further increasing thickness, d/R decreases. Eventually a neutral surface migrates to the front face and is lost. The cantilever continues to have only two neutral surfaces thereafter. Figure 7 shows how the neutral surfaces change with increasing thickness at fixed illumination $\alpha=5$, $\alpha/\beta=50$. Features are slightly shifted to smaller w in comparison with the $\beta=0$ case of [16]. With two regions of compression and two of elongation, one expects subtle behavior when considering compression-induced director rotation [25] in such cantilevers, to which we return elsewhere.

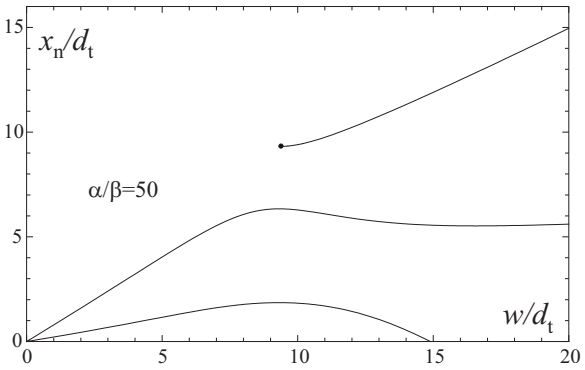

FIG. 7. Neutral surfaces for fixed incident light intensity $\alpha=5$, $\alpha/\beta=50$ as cantilever thickness w changes. At the w maximizing curvature, a third neutral surface appears from the rear face; at greater w a neutral surface is lost at the front face.

VI. TEMPERATURE EFFECTS

We have neglected the effect of heat generated by absorption of light. Gradients of optical intensity in the cantilever might be expected to generate gradients of temperature and thus of thermal contraction, leading to thermal bend. Experiments where polydomain elastomers bend in the direction of the polarization of light [11] show directly that optical effects dominate (see the analysis of polydomains in [12]) over thermal component of bend. We here quantify the relative size of optical and thermal effects. Let the temperature distribution in the beam be $\theta(x,t)$, and take the origin of the temperature scale to be such that the ambient temperature outside the cantilever is zero, $\theta=0$. The temperature distribution satisfies a continuity equation in which the heat flux contains the usual thermal gradient term $-\kappa\frac{\partial\theta}{\partial x}\hat{\mathbf{x}}$ and the divergence of the Poynting flux, $I(x)\hat{\mathbf{x}}$, is a source term,

$$C\frac{\partial\theta}{\partial t}-\kappa\frac{\partial^2\theta}{\partial x^2}=-I_0\frac{\partial\mathcal{I}}{\partial x}, \tag{24}$$

where C is the specific heat of the cantilever per unit volume and κ is the thermal conductivity perpendicular to the direc-

tor, that is along the normal to the flat surface of the cantilever. The diffusion coefficient D is given by the ratio κ/C. Typical values for elastomers are around $\sim 10^{-7}$ m^2 s^{-1} [26], with some anisotropy in D arising in nematic elastomers from anisotropy in the conductivity that we ignore here since thermal effects will in any case turn out to be small. The time taken for heat to diffuse across the thickness of the cantilever is $\approx w^2/D \sim 0.001$ s for a 10 μm sample [11,27]. For times significantly longer than this, one obtains the steady-state solution $\theta(x)$. At the front and back surfaces there are convective losses which are described by Newton's law of cooling, that is the heat flux carried away from a surface is $\delta\theta(0)$ (the temperature outside is $\theta=0$), where δ is the convective heat transfer coefficient. For free convection in air, $\delta \approx 5$ W m^{-2} K^{-1}. These convection losses are equal to the thermal flux of heat at the respective surfaces,

$$\theta(0) - \left.\frac{\kappa}{\delta}\frac{d\theta}{dx}\right|_{x=0} = 0,$$

$$\theta(w) + \left.\frac{\kappa}{\delta}\frac{d\theta}{dx}\right|_{x=w} = 0, \tag{25}$$

where the signs reflect the direction of the outward surface normal. The thermal conductivity is $\kappa \approx 0.2$ W m^{-1} K^{-1} [28]. The solution to Eq. (24) satisfying boundary conditions is

$$\frac{\theta(x)}{\bar{\theta}} = 1 - \frac{\left(1+\frac{\delta x}{\kappa}\right)}{\left(2+\frac{\delta w}{\kappa}\right)}\left(1+\mathcal{I}_w+\frac{\delta w}{\kappa}\int_0^1 \mathcal{I}(wy)dy\right) + \frac{\delta w}{\kappa}\int_0^{x/w} \mathcal{I}(wy)dy. \tag{26}$$

The characteristic temperature $\bar{\theta}=I_0/\delta$ is the temperature that the sample surface would need to attain in order to lose by Newton cooling all the heat equivalent to the incident Poynting energy. Both of the integrals appearing in this expression have been scaled such that their value is bounded by unity. The scale of their contributions is thus set by their prefactor $\delta w/\kappa$. This dimensionless quantity compares the thickness of the sample w with the thermal penetration length set by the boundary conditions κ/δ.

There are several interesting limits to this equation:

(i) Using the values for κ and δ given above and assuming a cantilever thickness $w \sim 10$ μm we obtain $\frac{\delta w}{\kappa} \approx 2.5 \times 10^{-4} \ll 1$, and thus the temperature distribution is essentially constant throughout the sample, that is,

$$\frac{\theta(x)}{\bar{\theta}} = \left(\frac{1-\mathcal{I}_w}{2}\right) + O(\delta w/\kappa). \tag{27}$$

A constant temperature through the sample leads to contraction along the long axis of the cantilever, but it will not induce bending, since this requires differential contractions. Therefore in this limit, which is close to experimental reality, bending effects in the steady state are due to the optical effects discussed previously, rather than heating.

(ii) Heat is produced proportionately to the rate optical intensity diminishes. There are regimes in which intensity $\mathcal{I}(x)$ decays linearly with depth into the cantilever, e.g., for $\alpha=10$, $\beta=0.2$, and $w \leq 8d_t$ in Fig. 2. For these conditions, that is where $d\mathcal{I}/dx=$const, then heat is generated at the same rate through the cantilever. In the steady state it diffuses to the surfaces, symmetrically if the surfaces are at the same temperature, and hence heat does not contribute at all to the bending. One sees this since now Eq. (26) becomes

$$\frac{\theta(x)}{\bar{\theta}} = \left(\frac{1-\mathcal{I}_w}{2}\right)\left[1+\frac{\delta w}{4\kappa}-\frac{\delta}{\kappa w}\left(x-\frac{w}{2}\right)^2\right], \tag{28}$$

a temperature distribution which is indeed symmetric about the midpoint of the cantilever. Since the thermally induced strains are also symmetric, they will not produce bending, although once again they will produce an overall contraction. If the cantilever thickness w is increased beyond the linear profile interval in, e.g., Fig. 2, then asymmetry in the heat production starts to occur, with less heat generated toward the back face. However, the magnitude of the asymmetry is reduced by diffusion and the thermal contribution to bend sets in only slowly with increasing w, see (i) above.

The neglect of heat is thus justified in two limits, first the convective heat losses from the boundary are likely to result in a uniform temperature distribution through the sample for experimentally realistic values of the thermal conductivity κ and the convective heat transfer coefficient δ. Further, in the regime of linear (i.e., nonexponential) decay of intense beams there is no thermal component of bend.

Thermal effects become more extreme, especially in elastomers, if an interior region of the cantilever's temperature exceeds the nematic-isotropic transition temperature. At this temperature an extremely large strain can develop in elastomers, and possibly in glasses. If it occurs in a region symmetrically disposed about the cantilever midplane, it could lead to pronounced contractions, but still not to bend. If it occurs in an asymmetrically disposed region, it could lead to large bends—an extreme case we return to in considering specifically elastomers and thus at the same time considering director rotation. Additionally one would there consider the displacement of neutral planes due to volumes of the cantilever suffering large contractions of their natural lengths.

VII. CONCLUSIONS

We have shown that nonlinear absorption (that is, nonexponential profiles) can be invoked to explain how bending can arise in cantilevers where, within Beer's law, one would otherwise expect no response. At high enough incident light intensities, there can be photobleaching and thereby penetration of radiation and thus elastic response even in cantilevers so heavily loaded with dye that the Beer penetration depth of the linear regime is insignificant compared with the cantilever's thickness. The nonlinear response in the high dye-loaded limit is possibly of the greatest experimental relevance. We have explored the roles of optically stimulated

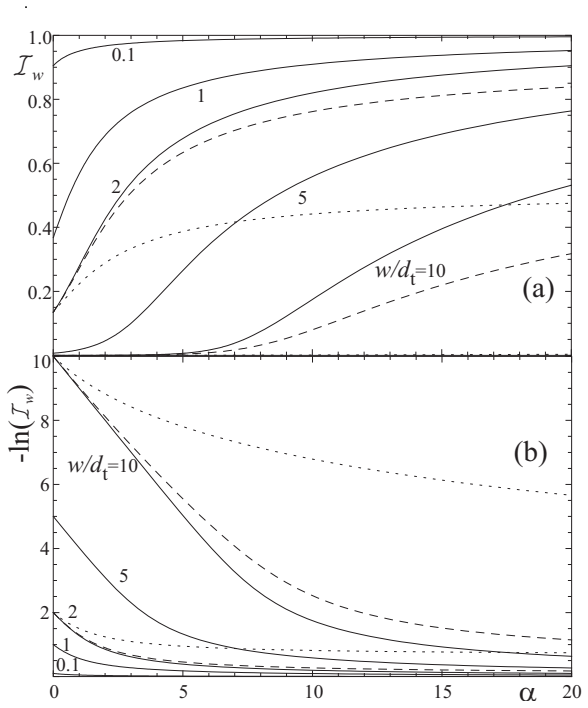

FIG. 8. (a) Scaled intensity at the back surface $\mathcal{I}_w$ as a function of the incident intensity α for various cantilever thicknesses w/d_t with $\beta=0$ (solid lines), and with $\alpha/\beta=50$ (dashed lines) and $\alpha/\beta=5$ (dotted lines) for two marked thicknesses. (b) Intensity plotted in the form of the absorbance $-\ln(\mathcal{I}_w)$ as a function of α with cantilever thicknesses and β values as in the upper figure.

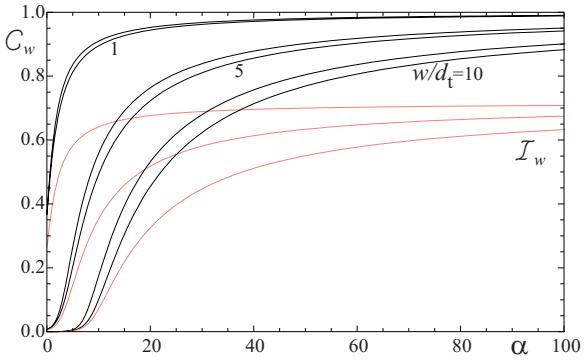

FIG. 9. (Color online) Corrected intensity at the back surface $\mathcal{C}_w$ as a function of the incident intensity α for various cantilever thicknesses w/d_t. In each case the upper curve is without host absorption, the lower with rather heavy host absorption such that $w/d_h=0.3$. For comparison, lower lighter lines, the corresponding uncorrected $\mathcal{I}_w$ curves are shown.

deexcitation of dyes and of optically generated heat in mechanical processes. Stimulated decay can be very important, but the role of heat seems minor.

An experiment [17] to explore the nonlinear absorption processes we have described measures the intensity emergent at the back surface for a sample of fixed width w illuminated at the front surface. Altering the incident intensity is equivalent to varying the parameter α. Taking a fixed depth (the thickness itself) w/d_t in Figs. 2 and 4 and increasing reduced incident power $\alpha=I_0/I_t$ is to take a slice through these figures to reveal increasing relative penetration, that is an increased reduced exit intensity $\mathcal{I}_w(\alpha)=I_w/I_0$, see Fig. 8(a). Scaling the output intensity by its incident value would produce a horizontal line $\mathcal{I}_w=\exp(-w/d_t)$ as a function of α for simple Beer-law attenuation; deviations from this line as power increases away from $\alpha=0$ are thus signs of non-Beer attenuation processes. In thin cantilevers $w/d_t=0.1$, $\mathcal{I}_w$ is close to unity, and only increases slowly as α is increased—for thin cantilevers nearly all of the incident flux is transmitted in any case. Conversely for thick cantilevers $w/d_t=10$ we see that there is very little transmittance for small α. For larger incident intensities, such that $\alpha \gtrsim 5$, the transmittance begins to increase rapidly with α—a consequence of the increased penetration due to nonlinear absorption processes. For two particular sample thicknesses, $\beta \neq 0$ cases are shown too. The curves show that a finite induced back-reaction rate reduces enhanced penetration, as one would expect. For the thickest sample, the higher β value is sufficient to effectively eliminate penetration of the beam. Deviation from Beer absorbance is perhaps better seen from plots of nonlinear absorbance itself, see Fig. 8(b). An experimental example, and its relation to their equivalent of our Eq. (6), is discussed at length by Statman and Janossy [17].

Despite host and dye absorptive processes being mixed in a nonlinear differential equation, an approximate allowance by division by the host transmittance seems to work well: $\mathcal{C}_w=\mathcal{I}_w/e^{-w/d_h}$ by substitution in Eq. (11) yields

$$\ln(\mathcal{C}_w)+\frac{1}{\psi}\ln\left(\frac{1+\psi(1+\alpha e^{-w/d_h}\mathcal{C}_w)}{1+\psi(1+\alpha)}\right)=-w/d_t. \quad (29)$$

We plot in Fig. 9 the corrected exit intensity $\mathcal{C}_w$ implied by (29). For very intense beams, $\alpha \gg 1$, the corrected intensity tends to 1. The dye is bleached and absorption is predominantly by the host. The true profile is then Beer-like and the correction is accurate. At lower intensities the correction is also seen to work surprisingly well. The upper of each curve for a given reduced thickness w/d_t is for no host absorption, representing the pure system being examined. The corrected curve (lower in each case) is close to the ideal curve, even for the very heavy absorption $w/d_h=0.3$ in the illustration. For smaller absorptions the corrected and the ideal curves are practically indistinguishable. Thus the straightforward correction method should give a good estimate of the underlying nonlinear absorptive processes.

Much of the discussion has been of intensities with reference to the ideal Beer intensity, for instance, Fig. 8(a). Beer behavior is obtained when intensities are low enough that the *trans* population is little reduced. This is also obtained at short times when as yet little conversion has taken place. An output power $\mathcal{I}_w=\exp(-w/d_t)$ must emerge and has the value of the vertical axis intercept in Fig. 8(a) (and is also the same as the reduced weak-beam emergent power). Thus, for a given power α and thickness w/d_t, the initial emergent power must rise to the higher value characteristic of the curve in question. The dynamics by which a spatial bleaching pattern is established is nonlinear and complicated, see comments below Eq. (4).

One can also propose that bleaching can lead to an emergent power that diminishes in time from the initial Beer value if the *cis* species have a higher absorption than the *trans*. A higher *cis* absorption arises if the incident light frequency is shifted to be closer to the *cis* absorption line. One can rearrange Eq. (6) by evaluating it at $x=w$ and noting that $-w/d_t=\ln(\mathcal{I}_B)$, where subscript B denotes the Beer, $t=0$ reduced intensity. Thus denoting by $\mathcal{R}$ the ratio $\mathcal{I}_w/\mathcal{I}_B$, one has

$$\ln(\mathcal{R}) = \frac{1-\alpha/(\eta\beta)}{(1+\eta)/\eta}\ln\left(\frac{1+\beta'\mathcal{I}_B R}{1+\beta'}\right). \tag{30}$$

It is evident that the ln on the right-hand side is always negative since $\mathcal{I}_B R=\mathcal{I}_w\leq 1$ and hence if $\alpha<\eta\beta$ then the left-hand side is also negative, that is $\mathcal{R}<1$—the intensity drops below the Beer value rather than rising with time and increasing power. The criterion, referring back to the ratio of the quantum efficiencies, amounts to $d_c<d_t$, that is, attenuation due to *cis* is greater than that due to *trans*. Sample thickness is encoded in $\mathcal{I}_B=\exp(-w/d_t)$. Solutions to Eq. (30) are shown in Fig. 10. Care is needed in interpreting this figure: As thickness increases, the absolute amount of light passing through the sample is greatly reduced since the Beer normalization to $\mathcal{I}_w$ in $\mathcal{R}$ is becoming exponentially small. This reverse effect of photobleaching is an example of the reverse saturation absorption (RSA) problem wherein an excited state cross section can be larger than that of the ground state, thus acting as a useful limiter of transmission of intense beams. The RSA problem has been extensively studied in the literature, see [29] and references therein.

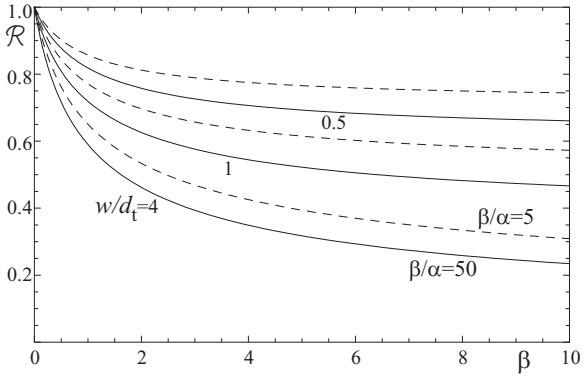

FIG. 10. Intensity at the back surface scaled by the Beer intensity expected at the back face, $\mathcal{R}=\mathcal{I}_w/\mathcal{I}_B$ as a function of the incident intensity scaled by the intensity characteristic of the *cis* state, that is $\beta=I_0/I_c$ for cantilever thicknesses $w/d_t=4$, 1, and 0.5 with $\beta/\alpha=50$ (solid) and $\beta/\alpha=5$ (dashed) pairs of lines for each thickness. The emergent intensity is lower than the Beer value, in contrast to the rest of the paper where bleaching enhances penetration.

ACKNOWLEDGMENTS

We are grateful for discussions with David Statman and Peter Palffy-Muhoray, and to the EPSRC-GB for funding.

[1] M. Warner and E. Terentjev, *Liquid Crystal Elastomers* (Oxford, New York, 2003), also revised paperback edition, 2007.
[2] G. Mol, K. Harris, C. Bastiaansen, and D. Broer, Adv. Funct. Mater. **15**, 1155 (2005).
[3] H. Finkelmann and H. Wermter, **219**, 189 (2000).
[4] A. Tajbakhsh and E. Terentjev, Eur. Phys. J. E **6**, 181 (2001).
[5] H. Finkelmann, E. Nishikawa, G. G. Pereira, and M. Warner, Phys. Rev. Lett. **87**, 015501 (2001).
[6] J. Cviklinski, A. R. Tajbakhsh, and E. M. Terentjev, Eur. Phys. J. E **9**, 427 (2002).
[7] C. van Oosten, K. Harris, C. Bastiaansen, and D. Broer, Eur. Phys. J. E **23**, 329 (2007).
[8] M. Camacho-Lopez, H. Finkelmann, P. Palffy-Muhoray, and M. Shelley, Nat. Mater. **3**, 307 (2004).
[9] K. Harris, R. Cuypers, P. Scheibe, C. van Oosten, C. Bastiaansen, J. Lub, and D. Broer, J. Math. Chem. **15**, 5043 (2005).
[10] N. Tabiryan, S. Serak, X.-M. Dai, and T. Bunning, Opt. Express **13**, 7442 (2005).
[11] Y. Yu, M. Nakano, and T. Ikeda, Nature (London) **425**, 145 (2003).
[12] D. Corbett and M. Warner, Phys. Rev. Lett. **96**, 237802 (2006).
[13] M. Warner and L. Mahadevan, Phys. Rev. Lett. **92**, 134302 (2004).
[14] M. Kondo, Y. Yu, and T. Ikeda, Angew. Chem. **45**, 1378 (2006).
[15] C. van Oosten, C. Bastiaansen, and D. Broer (private communication).
[16] D. Corbett and M. Warner, Phys. Rev. Lett. **99**, 174302 (2007).
[17] D. Statman and I. Janossy, J. Chem. Phys. **118**, 3222 (2003).
[18] C. Eisenbach, Polymer **21**, 1175 (1980).
[19] D. Corbett, M. Warner, and C. L. van Oosten, e-print arXiv:0712.1772v2.
[20] M. Hercher, Appl. Opt. **6**, 947 (1967).
[21] http://mathworld.wolfram.com/LambertW-Function.html
[22] C. Eisenbach, Makromol. Chem. **179**, 2489 (1978).
[23] M. Kryszewski, B. Nadolski, A. North, and R. A. Pethrick, **76**, 351 (1980).
[24] M. Abramovitz and I. Stegun, *Handbook of Mathematical Functions* (Dover, New York, 1972).
[25] R. Verduzco, G. Meng, J. A. Kornfield, and R. B. Meyer, Phys. Rev. Lett. **96**, 147802 (2006).
[26] A. W. Broerman, D. C. Venerus, and J. D. Scheiber, J. Chem. Phys. **111**, 6965 (1999).
[27] C. L. van Oosten, K. D. Harris, C. W. M. Bastiaansen, and D. J. Broer, Eur. Phys. J. E **23**, 329 (2007).
[28] Z. Q. Niu, Q. Y. Chen, S. Y. Shao, X. Y. Jia, and W. P. Zhang, J. Micromech. Microeng. **16**, 425 (2006).
[29] A. Kobyakov, D. Hagan, and E. van Stryland, J. Opt. Soc. Am. B **17**, 1884 (2000).